Resonant effects in a SQUID qubit subjected to nonadiabatic changes

F. Chiarello,[1] S. Spilla,[2,3,*] M. G. Castellano,[1] C. Cosmelli,[4] A. Messina,[2] R. Migliore,[5] A. Napoli,[2] and G. Torrioli[1]

[1]*IFN-CNR, via Cineto Romano 42, 00156 Rome, Italy*

[2]*Dipartimento di Fisica e Chimica, Università di Palermo, I-90123 Palermo, Italy*

[3]*Institut für Theorie der Statistischen Physik, RWTH Aachen University, D-52056 Aachen, Germany*

[4]*Dip. Physics, Università di Roma "Sapienza", 00185 Rome, Italy*

[5]*Institute of Biophysics, National Research Council via Ugo La Malfa 153, 90146 Palermo, Italy*

(Received 17 October 2013; revised manuscript received 12 March 2014; published 11 April 2014)

By quickly modifying the shape of the effective potential of a double SQUID flux qubit from a single-well to a double-well condition, we experimentally observe an anomalous behavior, namely, an alternation of resonance peaks, in the probability to find the qubit in a given flux state. The occurrence of Landau-Zener transitions as well as resonant tunneling between degenerate levels in the two wells may be invoked to partially justify the experimental results. A quantum simulation of the time evolution of the system indeed suggests that the observed anomalous behavior can be imputable to quantum coherence effects. The interplay among all these mechanisms has a practical implication for quantum computing purposes, giving a direct measurement of the limits on the sweeping rates possible for a correct manipulation of the qubit state by means of fast flux pulses, avoiding transitions to noncomputational states.

DOI: 10.1103/PhysRevB.89.134506 PACS number(s): 03.75.Lm, 03.65.−w, 02.60.Cb

I. INTRODUCTION

Superconducting devices based on the Josephson effect are an important testbed for investigating deep aspects of quantum mechanics such as macroscopic quantum phenomena [1–4] and circuit quantum electrodynamics (cQED) [5–10]. Such devices are moreover promising candidates for the practical implementation of solid-state quantum computing [11–20]. This is thanks to the possibility to arrange superconducting circuits in a desired way with great flexibility [21–23] and also because their behavior can be analyzed by means of equivalent mechanical models [24], describing the motion of fictitious particles moving in an effective potential, with a supposed quantum behavior at low temperature. For example, it is possible to realize Josephson anharmonic oscillators that can be used as artificial atoms, which can be manipulated by microwaves with NMR-like techniques [25], and which can also be coupled with superconducting resonators for single-photon experiments in cavities [5,6]. Moreover, it is often possible to control and modify the effective potential shape in time with a fast and accurate timing. This allows, for example, the observation of very fast coherent oscillations (up to 20 GHz) of the magnetic flux states in a SQUID (superconducting quantum interference device) qubit [26,27], obtained just by quickly and strongly modifying the effective potential shape (from a symmetric double well to a single well, and back to the double well). This is done by simply applying flux pulses, in the absence of microwaves. For this kind of manipulation, of great importance is the rapidity of the modification of the effective potential shape. For example, if we consider quantum computing applications, the manipulation must be fast enough in order to induce nonadiabatic Landau-Zener transitions between the first two energy levels (used as computational space), but also slow enough in order to avoid transitions to upper levels (noncomputational space). Fortunately, generally speaking this is possible thanks to an appropriate energy gap existing between the first couple of levels and the upper ones, but the transition rate is an aspect that must be accurately considered and calibrated [28].

In this work, we investigate experimentally and theoretically the effect of the speed of modification of the potential shape in a double SQUID flux qubit, presenting the experimental observation and the theoretical analysis of an interesting quantum effect due to the interplay of Landau-Zener transitions and resonant tunneling. A similar phenomenon has been studied in Refs. [29,30], even if in a different system and contest.

II. DOUBLE SQUID

The device we consider is the so-called double SQUID [31], consisting of a superconducting loop of inductance L interrupted by a dc SQUID, a second smaller superconducting loop of inductance l interrupted by two identical Josephson junctions, each of (nominally) identical critical current i_0 and capacitance c [Fig. 1(a)]. The dc SQUID behaves approximately like a single junction of capacitance $C = 2c$ and tunable critical current $I_0(\Phi_c) = 2i_0 \cos(\Phi_c/\Phi_B)$ (where $\Phi_B = \frac{\Phi_0}{2\pi}$, being $\Phi_0 = h/2e$ the flux quantum), which is controlled by a magnetic flux Φ_c applied to the small loop (this approximation holds if the loop is small enough, i.e., for $li_0 \ll \Phi_0$). Note that $I_0(\Phi_c)$ can also be negative, and in this case the dc SQUID behaves as a π junction. The double SQUID behavior can be controlled by two distinct magnetic fluxes, one applied to the large loop (Φ_x) and the second to the small one (Φ_c, previous mentioned). The SQUID dynamics can be described by an equivalent mechanical model, with effective mass $m = C\Phi_B^2$, effective position corresponding to the total magnetic flux threading the large loop (Φ), and potential

$$U = \frac{(\Phi - \Phi_x)^2}{2L} - I_0(\Phi_c)\Phi_B \cos\left(\frac{\Phi}{\Phi_B}\right). \qquad (1)$$

This effective potential can have one or two distinct wells, according to the adimensional parameter $\beta(\Phi_c) = 2\pi I_0(\Phi_c)L/\Phi_0$: in the particular case $\Phi_x = 0$, there will be a

*samuele.spilla@unipa.it

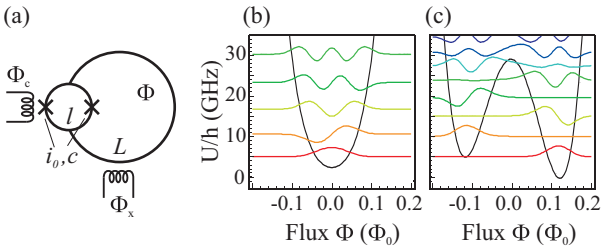

FIG. 1. (Color online) (a) Scheme of the double SQUID. (b) Effective potential of the double SQUID in the single-well case, with relative eigenwaves vertically shifted by the corresponding eigenenergies. (c) Double-well case with a slight asymmetry.

single well for $\beta > -1$ [approximately a harmonic potential with a characteristic frequency controlled by Φ_c, Fig. 1(b)], and two distinct wells separated by a barrier for $\beta < -1$ [with barrier height controlled by Φ_c, Fig. 1(c)]. The flux Φ_x controls the potential symmetry: for $\Phi_x = 0$ the potential is symmetric, otherwise it is tilted [Fig. 1(c)].

In order to study the effect of speed versus adiabaticity on the system, we concentrate our attention on a fast and large modification of the potential shape, from the single-well to the double-well case. This is just half of the complete manipulation of the qubit state presented in Refs. [26,27]. Initially, the system is maintained in the single-well case for a rest time t_w, waiting for the complete relaxation to the ground state. Then, it is moved rapidly to the double-well case, where a high barrier separates the two minima, and this is obtained by changing the control flux Φ_c with a characteristic sweeping rate $\chi = \frac{d\Phi_c}{dt}$. Finally, a readout of the SQUID flux state is done, corresponding to observe which of the two minima is occupied at the end. This is performed by an inductively coupled readout SQUID used as a magnetometer by means of measurements of the switching current [32]. The sequence is repeated many times in order to estimate the occupation probability P of the final flux (for example, the probability to obtain a final right flux state). The complete operation is repeated for different unbalancing fluxes Φ_x. For slow (adiabatic) modifications we expect that the system remains always in its ground state: the left flux state when the left minima is the lower one (for $\Phi_x < 0$), and the right flux state in the opposite case (for $\Phi_x > 0$), with a sweet transition between these opposite cases around the symmetry point ($\Phi_x \approx 0$). In this case, the probability P as a function of the unbalancing flux Φ_x presents a sigmoidal shape. By increasing the sweeping rate χ, we expect an excitation of upper levels due to nonadiabatic transitions, with a possible emerging of effects related to this population.

III. EXPERIMENTAL SETUP AND RESULTS

We performed the measurements on devices realized by standard trilayer Nb/AlOx/Nb technology, with nominal parameters $L = 85pH, l = 7pH, I_0 = 8\mu A$, and $c = 0.3pF$, in a dilution refrigerator with base temperature $T = 30$ mK arranged for ultralow noise qubit measurements (μ metal, superconducting and normal metal shields, thermocoax and L-C-L filters on dc lines, different attenuator stages on the

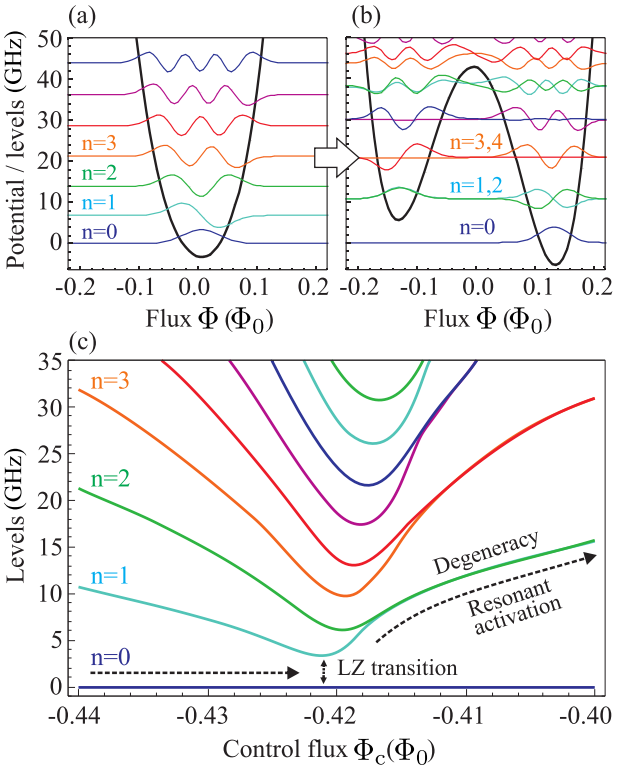

FIG. 2. (Color online) (a) Energy potential of the system and relative eigenstates in the single-well case (for $\Phi_c = -429$ mΦ_0). (b) Energy potential of the system and relative eigenstates in the double-well case (for $\Phi_c = -412$ mΦ_0), with a slight asymmetry ensuring the degeneracy (for $\Phi_x = 0.543$ mΦ_0). (c) Variation of the energy levels positions for different fluxes Φ_c (for $\Phi_x = 0.543$ mΦ_0). Note that for convenience all energies are expressed as frequencies in GHz, and are shifted by subtracting the ground-state energy.

signal line). A preliminary study of the switching current in the readout dc SQUID gives an escape temperature of about 250 mK, compatible with the crossover temperature within the experimental errors. This indicates the absence of an excess temperature due to noise [32]. The probability P is evaluated by repeating the preparation-modification-readout cycles for 1000 times at a rate of 10 kHz. The initial preparation is obtained by waiting for a time $t_w = 200$ ns in the single-well condition [Fig. 2(a)], for $\Phi_c \approx -480$ mΦ_0. In this condition, the system is well approximated by a harmonic oscillator with characteristic frequency $\approx$19 GHz, corresponding to a level spacing of about 0.91 K, very high with respect to the thermal bath temperature, so that we expect a negligible thermal excitation.

The potential shape modification is driven by a fast pulse generator, presenting signals with a typical rise time $t_R = 0.8$ ns that can be changed by using homemade tunable L-C-L filter. The modified pulse is fully characterized thanks to a fast oscilloscope, in particular, it is possible to check the pulse shape and the actual rise time. The fast signal is transmitted to the device thanks to a 50-Ω matched coaxial cable interrupted by three 20-dB attenuators placed at 300-K, 1-K, and 30-mK stages. More details on the setup can be found in Ref. [26]. We tested the entire line at room temperature and in the absence of the chip, while the present setup does not allow to test the entire

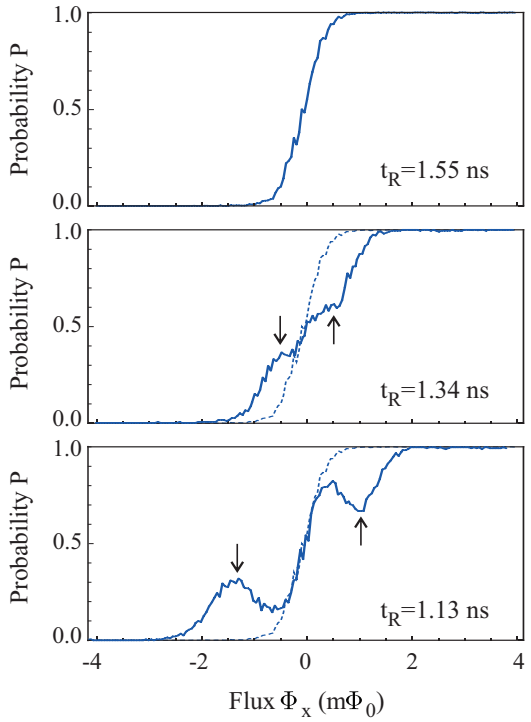

FIG. 3. (Color online) Experimental results for the probability P to measure a right flux state for different unbalancings Φ_x at three different rise times t_R. Resonance peaks are visible for faster transitions (arrows in second and third plots)

system (line plus chip) at low temperature. For this reason, we can expect a large error in the determination of the real signal shape and rise time at the device level. The applied signal modifies the potential from the single-well condition, at $\Phi_c \approx -480\ \mathrm{m}\Phi_0$, to the double-well case, at $\Phi_c \approx -360\ \mathrm{m}\Phi_0$, passing through the critical condition $\Phi_c \approx -422\ \mathrm{m}\Phi_0$ where there is the transition between the single-well and double-well conditions (Fig. 2). At the end of each cycle, the final flux state is measured by the coupled readout dc SQUID. This is done by applying a current ramp to the SQUID and recording the switching current, which is directly related to the qubit flux. The sequence is repeated for different unbalancing fluxes Φ_x, ranging from $-4\ \mathrm{m}\Phi_0$ to $+4\ \mathrm{m}\Phi_0$, obtaining the probability curves plotted in Fig. 3. These curves are obtained for three different rise times: 1.55, 1.34, and 1.13 ns. In the top plot, we observe the sigmoidal function expected for a slow rate. In the middle and lower plots, two distinct order of peaks appear, respectively, at about $\pm 0.55\ \mathrm{m}\Phi_0$ and $\pm 1.1\ \mathrm{m}\Phi_0$. The measurement can be repeated for different rise times obtaining the three-dimensional (3D) curve shown in Fig. 4.

From Fig. 4 we can note some enlightening characteristics. First of all, the position of peaks (in Φ_x) corresponds to the conditions for which different levels in the two wells are aligned (degenerate) [Fig. 2(b)]. This strongly suggests that the presence of peaks is a manifestation of resonant tunneling between wells. Second, we note that the appearing of peaks requires rise times below a particular critical value, namely, it is necessary to have a high enough sweep rate in order to observe peaks. Third, there is an alternation of peaks' orders: when the second order of peaks appears, the first order

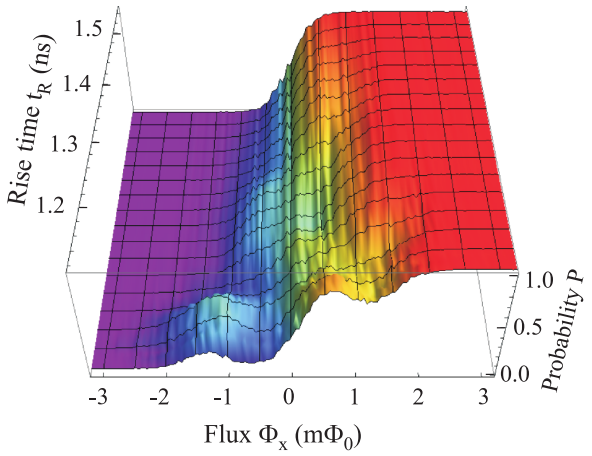

FIG. 4. (Color online) Experimental results for the probability P to measure a right flux state for different unbalancings Φ_x at different rise times t_R, plotted as a 3D surface.

disappears. In Fig. 2(c), it is plotted the modification of the first nine energy levels in the passage from the single-well to the double-well condition (in the degenerate case for $\Phi_x = 0.55\ \mathrm{m}\Phi_0$). This figure can help us in a qualitative explanation of the observed peaks. In the single-well condition (on the left), it appears reasonable to suppose that only the ground state is populated. Close to the critical point $\Phi_c \approx -0.42\ \Phi_0$, where the barrier appears to separate two distinct wells, Landau-Zener transitions populate the upper levels, with an efficiency depending on the sweep rate $\frac{d\Phi_c}{dt}$. These excited states can cross the barrier thanks to a resonant tunneling when the alignment condition is met. The experimental results thus suggest that these two effects combine together and produce the observed peaks, due to an excess of population in the upper well when the resonant and the nonadiabatic conditions are both fulfilled. The region where this effect is active is small, of the order of $\frac{1}{10}$ of the entire span of the flux Φ_c ($120\ \mathrm{m}\Phi_0$), and this region is crossed in a similar fraction of the entire rise time duration, about 0.1 ns. We stress again that the combination of Landau-Zener and resonant tunneling can explain the first two observations (position of peaks and appearance of them only below a critical rise time), but not the third one, that is, the alternation of peaks' orders.

IV. SIMULATIONS AND DISCUSSIONS

In order to gain information about possible physical mechanisms and/or properties of the system which may be responsible for the appearance of the alternation of peaks' order as in Fig. 4, in what follows we develop a more quantitative analysis exploiting a simple quantum model useful to describe the system under scrutiny. To do this, we start considering the Hamiltonian model relative to the potential (1), rewritten in a more convenient way:

$$H(t) = -\frac{1}{2m}\frac{\partial^2}{\partial\varphi^2} + m\Omega^2\frac{(\varphi-\varphi_x)^2}{2} + m\Omega^2\beta(t)\cos(\varphi), \quad (2)$$

where $\Omega = 1/\sqrt{LC}$, $\varphi = \Phi/\Phi_B$, and $\varphi_x = \Phi_x/\Phi_B$. Moreover, $\beta(t) = -I_0[\Phi_c(t)]\frac{\Phi_B}{m\Omega^2}$. The Hamiltonian (2) is well

suited to describe the time evolution of a particle in one-dimensional time-dependent potential. In particular, appropriately choosing the function $\beta(t)$, it is possible to vary the potential shape going, in an interval of time $\tilde{t}$, from a single to a double well, thus reproducing the initial and final conditions of the experiment discussed before. The problem therefore consists in finding, as a function of both the unbalancing parameter φ_x as well as of the rise time t_R, the probability P that, at the end of the process, the particle is found in the right well. Let us observe that knowing the state of the system $|\Psi(\tilde{t})\rangle$ at the time instant $\tilde{t}$, this probability can be simply evaluated as

$$P = \int_{\text{right well}} \Psi^*(\tilde{t})\Psi(\tilde{t})d\varphi. \tag{3}$$

Let us indicate by $|\psi_n(t)\rangle$ a set of instantaneous eigenfunctions of the Hamiltonian (2):

$$H(t)\,|\psi_n(t)\rangle = E_n(t)\,|\psi_n(t)\rangle. \tag{4}$$

Exploiting these states, we can write

$$|\Psi(t)\rangle = \sum_{n=0}^{\infty} \exp\left[i\int_0^t E_n(\tau)d\tau\right] s_n(t)\,|\psi_n(t)\rangle, \tag{5}$$

where the function $s_n(t)$ is a solution of the following set of integrodifferential equations:

$$\dot{s}_n(t) = -\sum_{k=0}^{\infty} M_{nk}(t) \exp\left[i\int_0^t [E_n(\tau) - E_k(\tau)]d\tau\right] s_k(t) \tag{6}$$

with $M_{nk}(t) = \langle\psi_n(t)|\,\dot{\psi}_k(t)\rangle$. Starting from Eqs. (3) and (5), the probability P can be then written as

$$\begin{aligned} P &= \sum_{n=0}^{\infty} |s_n(\tilde{t})|^2 \int_{\text{right well}} \psi_n^*(\tilde{t})\psi_n(\tilde{t})d\varphi \\ &\equiv \sum_{n=0}^{\infty} |s_n(\tilde{t})|^2 L_n \end{aligned} \tag{7}$$

with

$$L_n = \int_{\text{right well}} \psi_n^*(\tilde{t})\psi_n(\tilde{t})d\varphi. \tag{8}$$

An exact analytical resolution of the coupled integrodifferential equations (6) is not easy. Thus, we proceed further by performing numerical simulations of the dynamical behavior of the system, carefully taking into account both the nonadiabaticity in the system dynamics and the possible emergence of resonant tunneling processes. As a first step, considering $\beta(t)$ as a parameter, we numerically diagonalize the Hamiltonian (2) at a generic time instant t, finding its instantaneous eigenvectors $|\psi_n(t)\rangle$ and the corresponding eigenvalues $E_n(t)$.

Considering values of t_R of interest in the context of this paper, we have evaluated the quantity L_n, defined in Eq. (8), in correspondence to different values of n verifying, as expected, that, at least for not too large n, L_n is almost equal to one or negligible, witnessing that the first eigenstates are practically localized for $\Phi_x \neq 0$. In our simulation, however, we use the numerical value of L_n instead of 0 or 1.

To evaluate the probability P, we thus need to calculate the populations $|s_n(\tilde{t})|^2$ by numerically solving the system (6) explicitly giving the way in which the potential shape modifies itself going from the initial condition to the final one during the time $\tilde{t}$. In other words, we now have to choose the function $\beta(t)$ appearing in Eq. (2). We wish to underline that this is a very delicate point. It is undoubted, indeed, that the dynamics of the system will be deeply affected from the way of varying the potential shape. Thus, we expect to find different results in correspondence to a different choice of $\beta(t)$.

A sigmoidal function allows a simple and reasonable description, at least from a qualitative point of view because of experimental uncertainties on the exact $\beta(t)$ shape as discussed in Sec. III. Thus, we fix it as $\beta(t) = \beta(0)[1 - \zeta(t)] + \beta(\tilde{t})\zeta(t)$ with $\zeta(t) = \frac{Erf[(2t/\tilde{t}-1)w-s]-Erf(-w-s)}{Erf(w-s)-Erf(-w-s)}$, $Erf(x) = \frac{2}{\sqrt{\pi}}\int_0^x e^{-t^2}dt$, choosing in particular $w = 2$ and $s = 0.3$. It is the case to stress that varying these two parameters implies, as a consequence, a changing in the rise time t_R. In order to investigate the appearance of peaks in Fig. 4, we have calculated the probability of finding the particle in the right well for different values of $\Phi_x = \varphi_x\Phi_B$ supposing, as it appears physically reasonable, that at $t = 0$ the system is in its ground state. In particular, we evaluated such a probability considering a range of Φ_x in correspondence of which peaks appear, as suggested by the experimental data. Considering values of t_R as in Fig. 4, our simulation does not evidence the existence of significant peaks. However, taking into account the fact that the peaks in the probability P arise reducing the rise time and in view of the experimental uncertainties discussed before, we have simulated the behavior of the system exploring smaller t_R. The results obtained are reported in Fig. 5 where the probability P is plotted as function of both Φ_x and t_R.

As expected, peaks of resonance appear in correspondence to different values of Φ_x. However, the position of such peaks with respect to the rise time t_R does not reflect, not only quantitatively but also qualitatively, the experimental observations. In other words, even if a dependence of P on t_R is evident, the function $P(t_R)$ is very different from the experimental one. In particular, the probability P obtained by

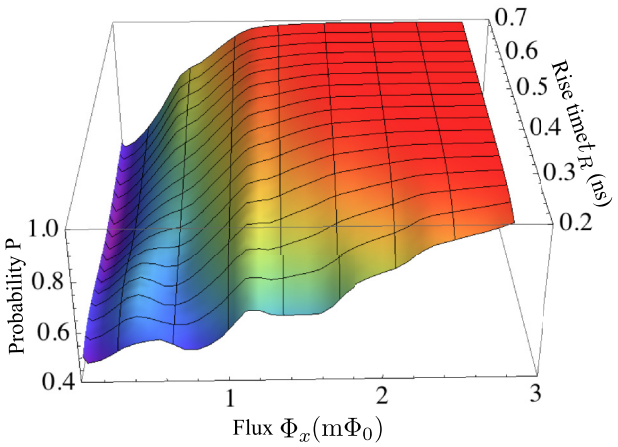

FIG. 5. (Color online) Probability P to find the system in the right well against the unbalancing Φ_x and rise time t_R, supposing that at $t = 0$ it is in its ground state.

simulation (see Fig. 5) is not characterized by the alternation of peaks' order as in Fig. 4. Such a result, moreover, does not seem to be imputable to the particular choice of the $\beta(t)$ we made. We have indeed verified that this is the case by choosing a linear function and obtaining the same qualitative behavior of that shown in Fig. 5. If it is true that the manner in which we modify the potential shape deeply affects the dynamics of the system and thus the probability P that the system is found in the right well at the end of the potential modification, another key ingredient to be considered is surely the state of the system at $t = 0$. Taking into account the fact that the temperature at which the experiment is performed is $\sim$30 mK, it is reasonable to suppose that at $t = 0$ there is a small, but not zero (of the order of few percent), probability that the system is in its first excited state. Thus, it could be reasonable to assume that the preparation step leaves the system in a mixture $\rho = x^2 |\psi_0(0)\rangle \langle\psi_0(0)| + (1 - x^2) |\psi_1(0)\rangle \langle\psi_1(0)|$ of the ground and the first excited states. Performing simulation starting from this mixture instead of the ground state, we have verified that, considering values of x compatible with $T \simeq 30$ mK, we do not get significant differences with respect to the results displayed in Fig. 5. We have also checked that increasing the relative weight x of the first excited state in the initial mixture worsens the accordance between theoretical predictions and experimental results. The theoretical prediction instead drastically changes if we suppose that quantum coherences are present in the initial state of the system. Such an assumption can be justified by considering the fact that the waiting interval of time t_w was not long enough to allow the complete destruction of the coherences between the ground and the first excited states of the double SQUID. If this is the case, it is reasonable to assume that at $t = 0$ the system is in a quantum superposition $|\Psi(0)\rangle = x |\psi_0(0)\rangle + \mathbf{e}^{i\theta}\sqrt{(1 - x^2)} |\psi_1(0)\rangle$ of the first two low-lying states, instead of a mixture of the two states as supposed before. Starting from this initial state, the probability P shows a dependence on both Φ_x and t_R as displayed in Fig. 6 where we have considered a smaller range of t_R to better appreciate the behavior of P. As expected, also in view of experimental uncertainties on the $\beta(t)$ function as well as on the parameters defining the system, Fig. 6 does not exactly match the experimental results presented before, even if the qualitative behavior of P seems to be well reproduced. More in detail, the most important aspect of the results shown in Fig. 6 consists in the fact that, as experimentally observed, there is an alternation of the peaks' order determined by both the asymmetry in the potential governed by the value of the unbalancing parameter Φ_x, and on the rise time t_R required to go from a single to a double well. The theoretical analysis developed in this paper has the merit to disclose the role played by the persistence of quantum coherences in the initial state of the double SQUID. We wish to stress indeed that starting from an initial state as the ground state of the qubit or a mixture of the same ground state and the first excited one, even if leading to the appearance of peaks, is completely unable to predict the alternation of minima and maxima as requested by the experimental results. Thus, our assumption, that is the persistence of quantum coherences, leads to predictions in good qualitative agreement with the experimental results. The intriguing

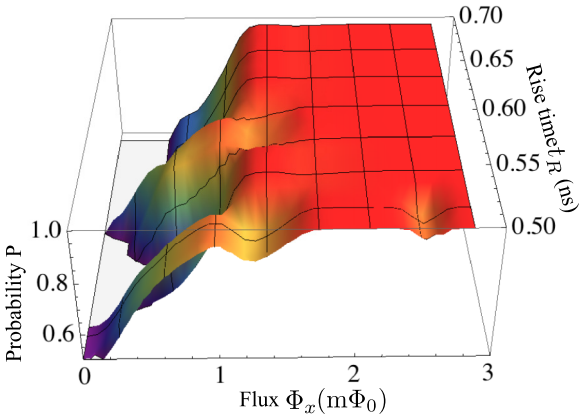

FIG. 6. (Color online) Probability P to find the system in the right well against the unbalancing Φ_x and rise time t_R, supposing that at $t = 0$ it is in the linear superposition $|\Psi(0)\rangle = x |\psi_0(0)\rangle + \mathbf{e}^{i\theta}\sqrt{(1 - x^2)} |\psi_1(0)\rangle$ of its ground and first excited states in correspondence to $x = 0.95$ and $\theta = 0$.

point is that all the alternative (seemingly more reasonable) assumptions concerning the initial state of the SQUID predict a behavior not compatible with some aspect of the observed one.

Before concluding, we comment about possible decoherence effects in the dynamical behavior of the system. It is important to underline that, as we have previously discussed, the temporal interval where the physical mechanisms at the basis of the observed effects are active is a small fraction (of the order of 0.1 ns) of the total duration of the experiment (about 1 ns). As a first approximation, it is thus reasonable to neglect decoherence effects in the system dynamics, which present time scales of the order of nanoseconds. Anyway, it is the case to underline that in this context the source of noise is the $\frac{1}{f}$ noise [33] that generally speaking acts modifying the effective control parameter as, for example, Φ_x [34–36]. We thus expect that the effects of such a noise on the results reported in Fig. 6 would consist at most in a broadening of the observed peaks.

Summarizing, we have experimentally verified that a fast modification of the potential shape of a double SQUID gives rise to the activation of quantum resonance phenomena manifesting themselves as peaks in the probability of measuring a right flux state of the SQUID at the end of the nonadiabatic transition. The theoretical analysis we have performed seems moreover to lead to the conclusion that the characteristic behavior of such a probability is also a direct consequence of the presence of quantum coherences in the initial state of the system. This fact suggests to perform other experiments on the system under scrutiny aimed at revealing quantum interference effects in the behavior of some no-diagonal physical observables.

ACKNOWLEDGMENTS

The authors thank E. Safonov for stimulating and deep discussions on the subject of this paper. Financial support from the Italian Project PRIN 2008C3JE43_003 is acknowledged.

[1] M. Ansmann, H. Wang, R. C. Bialczak, M. Hofheinz, E. Lucero, M. Neeley, A. D. O'Connell, D. Sank, M. Weides, J. Wenner, A. N. Cleland, and J. M. Martinis, Nature (London) **461**, 504 (2009).

[2] V. Corato, E. Esposito, C. Granata, A. Monaco, B. Ruggiero, M. Russo, L. Stodolsky, and P. Silvestrini, IEEE Trans. Appl. Supercond. **11**, 994 (2001).

[3] C. Cosmelli, M. G. Castellano, R. Leoni, R. Torrioli, P. Carelli, and F. Chiarello, Supercond. Sci. Technol. **14**, 1031 (2001).

[4] C. H. van der Wal, A. C. J. ter Haar, F. K. Wilhelm, R. N. Schouten, C. J. P. M. Harmans, T. P. Orlando, Seth Lloyd, and J. E. Mooij, Science **290**, 773 (2000).

[5] A. Wallraff, D. I. Schuster, A. Blais, L. Frunzio, R.-S. Huang, J. Majer, S. Kumar, S. M. Girvin, and R. J. Schoelkopf, Nature (London) **431**, 162 (2004).

[6] R. Migliore and A. Messina, Eur. Phys. J. B **34**, 269 (2003).

[7] A. V. Dodonov, R. Lo Nardo, R. Migliore, A. Messina, and V. V. Dodonov, J. Phys. B: At., Mol. Opt. Phys. **44**, 225502 (2011).

[8] D. J. Egger and F. K. Wilhelm, Phys. Rev. Lett. **111**, 163601 (2013).

[9] T. Niemczyk, F. Deppe, H. Huebl, E. P. Menzel, F. Hocke, M. J. Schwarz, J. J. Garcia-Ripoll, D. Zueco, T. Hümmer, E. Solano, A. Marx, and R. Gross, Nat. Phys. **6**, 772 (2010).

[10] A. Blais, R. S. Huang, A. Wallraff, S. M. Girvin, and R. J. Schoelkopf, Phys. Rev. A **69**, 062320 (2004).

[11] M. D. Reed, L. DiCarlo, S. E. Nigg, L. Sun, L. Frunzio, S. M. Girvin, and R. J. Schoelkopf, Nature (London) **482**, 382 (2012).

[12] S. Aldana, Y. D. Wang, and C. Bruder, Phys. Rev. B **84**, 134519 (2011).

[13] R. Migliore, M. Scala, A. Napoli, K. Yuasa, H. Nakazato, and A. Messina, J. Phys. B: At., Mol. Opt. Phys. **44**, 075503 (2011).

[14] S. Spilla, R. Migliore, M. Scala, and A. Napoli, J. Phys. B: At., Mol. Opt. Phys. **45**, 065501 (2012).

[15] B. Ruggiero, P. Delsing, C. Granata, Y. Pashkin, and P. Silvestrini, *Quantum Computing in Solid State Systems* (Springer, Berlin, 2006).

[16] J. H. Plantenberg, P. C. de Groot, C. J. P. M. Harmans, and J. E. Mooij, Nature (London) **447**, 836 (2007).

[17] Matthias Steffen, Physics **4**, 103 (2011).

[18] Y. Makhlin, G. Schön, and A. Shnirman, Rev. Mod. Phys. **73**, 357 (2001).

[19] M. J. Everitt, T. D. Clark, P. B. Stiffell, A. Vourdas, J. F. Ralph, R. J. Prance, and H. Prance, Phys. Rev. A **69**, 043804 (2004).

[20] L. DiCarlo, M. D. Reed, L. Sun, B. R. Johnson, J. M. Chow, J. M. Gambetta, L. Frunzio, S. M. Girvin, M. H. Devoret, and R. J. Schoelkopf, Nature (London) **467**, 574 (2010).

[21] A. B. Zorin and F. Chiarello, Phys. Rev. B **80**, 214535 (2009).

[22] M. G. Castellano, F. Chiarello, R. Leoni, F. Mattioli, G. Torrioli, P. Carelli, M. Cirillo, C. Cosmelli, A. de Waard, G. Frossati, N. Grønbech-Jensen, and S. Poletto, Phys. Rev. Lett. **98**, 177002 (2007).

[23] V. I. Shnyrkov, A. A. Soroka, and S. I. Melnyk, Low. Temp. Phys. **34**, 610 (2008).

[24] A. Barone and G. Paternò, *Physics and Applications of the Josephson Effect* (Wiley, New York, 1982).

[25] J. M. Martinis, S. Nam, J. Aumentado, and C. Urbina, Phys. Rev. Lett. **89**, 117901 (2002).

[26] M. G. Castellano, F. Chiarello, P. Carelli, C. Cosmelli, F. Mattioli, and G. Torrioli, New J. Phys. **12**, 043047 (2010).

[27] S. Poletto, F. Chiarello, M. G. Castellano, J. Lisenfeld, A. Lukashenko, C. Cosmelli, G. Torrioli, P. Carelli, and A. V. Ustinov, New J. Phys. **11**, 013009 (2009).

[28] M. G. Castellano, F. Chiarello, and G. Torrioli, J. Supercond. Novel Magn. **24**, 1053 (2011).

[29] P. Silvestrini, B. Ruggiero, and Y. N. Ovchinnikov, Phys. Rev. B **54**, 1246 (1996).

[30] R. Rouse, S. Han, and J. E. Lukens, Phys. Rev. Lett. **75**, 1614 (1995).

[31] F. Chiarello, Eur. Phys. J. B **55**, 7 (2007).

[32] C. Cosmelli, P. Carelli, M. G. Castellano, F. Chiarello, R. Leoni, and G. Torrioli, IEEE Trans. Appl. Supercond. **11**, 990 (2001).

[33] F. Chiarello, E. Paladino, M. G. Castellano, C. Cosmelli, A. D'Arrigo, G. Torrioli, and G. Falci, New J. Phys. **14**, 023031 (2012).

[34] F. Yoshihara, K. Harrabi, A. O. Niskanen, Y. Nakamura, and J. S. Tsai, Phys. Rev. Lett. **97**, 167001 (2006).

[35] R. C. Bialczak, R. McDermott, M. Ansmann, M. Hofheinz, N. Katz, E. Lucero, M. Neeley, A. D. O'Connell, H. Wang, A. N. Cleland, and J. M. Martinis, Phys. Rev. Lett. **99**, 187006 (2007).

[36] O. Astafiev, Y. A. Pashkin, Y. Nakamura, T. Yamamoto, and J. S. Tsai, Phys. Rev. Lett. **96**, 137001 (2006).